

N O T I C E

THIS DOCUMENT HAS BEEN REPRODUCED FROM
MICROFICHE. ALTHOUGH IT IS RECOGNIZED THAT
CERTAIN PORTIONS ARE ILLEGIBLE, IT IS BEING RELEASED
IN THE INTEREST OF MAKING AVAILABLE AS MUCH
INFORMATION AS POSSIBLE

"Made available under NASA sponsorship
in the interest of early and wide dis-
semination of Earth Resources Survey
Program information and without liability
for any use made thereof."

Original photography may be purchased from
EROS Data Center

Sioux Falls, SD 57198

80-10006

CR-142383

MAPPING THERMAL INERTIA, SOIL MOISTURE AND EVAPORATION FROM AIRCRAFT DAY AND NIGHT THERMAL DATA

J. Dejae and J. Mégier

M. Kohl, G. Maracci, P. Reiniger and G. Tassone

Commission of the European Communities, Joint Research Centre, Ispra Establishment, Italy

J. Huygen

on fellowship from Agricultural University, Wageningen, The Netherlands, at J.R.C. Ispra

ABSTRACT

A multiple search and interpolation method has been developed in order to use the "Tell-us" model to map thermal inertia, soil moisture and cumulative daily evaporation by starting from thermal and visible data acquired by air borne scanner. Interpolations are made within and between look-up tables generated previously by the model which uses a reverse temperature simulation process.

After the necessary geometric, radiometric and atmospheric corrections have been applied, the scanner data are processed together with ground and meteorological data to produce moisture and evaporation maps. Comparison with available measurements indicates a tendency to underestimate soil moisture content; a similar trend seems to be also verified for cumulative daily evaporation. Mapping of locally non-homogeneous areas encounters some difficulties which are discussed.

1. INTRODUCTION

The Joint Research Centre Ispra is carrying out, within the "Tellus" project, an investigation in collaboration with laboratories from the whole European Community on the application of HCMM satellite thermal data for soil moisture and heat budget evaluation in zones of agricultural and environmental interest [1]. In this framework, the so-called "Tell-us" model has been developed for bare and sparsely vegetated areas, which uses separately the day and night temperatures T_d and T_n at the same geographical point, rather than their difference $T_d - T_n$, to determine thermal inertia, soil moisture and cumulative daily evaporation.

The "Tell-us" model will not be presented and discussed here as this has already been done [1]. The paper will rather describe the data processing methods used to handle the model in conjunction with the ground, meteorological and scanner data acquired during a joint flight performed on September 13, 1977, to the north west of London, U.K.

These data are suitable for a detailed application of the model as a preparation to the use of HCMM data on a wider scale. The purpose is to reach to a point by point mapping of soil moisture and evaporation by starting from pixel by pixel values of day and night temperatures and albedo, processed together with ground and meteorological data varying on a field by field basis or constant all over the flight strip.

The process must take into account many correcting procedures: correction of scan angle effect on the spectrometric values, correction of atmosphere effect, geometrical corrections on the night thermal data in order to achieve superposition with the day visible and thermal data.

As a result, moisture and evaporation maps are constructed and it will be possible to evaluate their reliability, rather for relative values actually (general trends and behaviour intra- and interfield) than for absolute values, due to the lack of sufficient ground measurements at this stage of the research. Obviously, the data processing scheme is independent of the intrinsic performances of the model and each further improvement of the latter should bring some corresponding improvement in the thematic maps produced.

2. THE DATA AVAILABLE - BRIEF OUTLOOK OF THE JOINT FLIGHT EXPERIMENT

This experiment was carried out on September 13, 1977, on the Grendon Underwood Experimental Catchment, north west of London. A data strip 8 km long and 1.6 km wide was acquired from 1000 m altitude with a Daedalus DS 1750 air-borne scanner at night-time minimum (5.43 am) and day-time maximum (2.00 pm) surface temperature. The thermal band of the scanner is between 8 and 14 μ m, the visible and near IR bands are given in Table 1. The ground resolution is 2.5 m at nadir. Night and day were clear and practically without clouds, with wind 0.2 m/s at night passage and 1.7 m/s at day passage (measured at 20 cm above ground level).

REPRODUCIBILITY OF THE
ORIGINAL PAGE IS POOR

(80-10006) MAPPING THERMAL INERTIA, SOIL
MOISTURE AND EVAPORATION FROM AIRCRAFT DAY
AND NIGHT THERMAL DATA (Commission of the
European Communities) 10 p HC A02/MF A01

N80-12522

CSCL 08G G3/43

Unclas
00006

24001-08

Simultaneously with the overflights, ground surface temperatures were measured with a PRT-5 radiometer with band 9.5 - 11.5 μm and 8 core samples were taken in a ploughed field (bare soil) of Denchworth clay at 15 cm depth, for moisture determination.

Air temperature, humidity and pressure were measured at various altitudes with a tethered balloon, 40 km from the site, to be used for atmospheric effect determination.

3. HANDLING OF THE "TELL-US" MODEL TO PRODUCE POINT BY POINT MAPS

3.1 Search and interpolation procedures within the Tell-us look-up table

To apply the Tell-us model, an algorithm was developed [1] which calculates, for a given set of input parameters, a graph in the night temperature and day temperature coordinates (Fig. 1a) made up of equi-thermal inertia and equi-relative surface humidity curves crossing each other. Each couple of measured day and night temperatures results in a point contained within one of the irregular quadrilaterals of this lattice; the corresponding thermal inertia (THI) and relative surface humidity (RSH) values can then be determined by constructing the interpolated equi-THI and equi-RSH passing through the point. A second graph of equi-THI curves, in RSH and cumulative daily evaporation (CDE) coordinates (Fig. 1b), allows the calculation of CDE by starting from the already known RSH and the proper interpolated equi-THI corresponding to the THI value calculated in the first graph.

A set of routines has then been written, which perform the following sequence of actions for each (Td, Tn) couple of the thermal scanner data:

- localize the quadrilateral containing the point in Td, Tn coordinates (Fig. 1a);
- construct the interpolated equi-THI and equi-RSH passing through the point;
- determine THI and RSH values by linear interpolation between neighboring values;
- construct the useful segment of the interpolated curve in the second graph (Fig. 1b) by linear interpolation between the upper and lower bounding equi-THI;
- determine the CDE value by linear interpolation within this segment.

The foresaid procedure leads in fact to search and interpolating routines within a complex table with two entries (RSH and THI) and three values (Td, Tn, CDE) at each entry crossing.

3.2 Various classes of input data - Interpolation between look-up tables

The input data required by Tell-us can be listed in the following way according to their various acquisition rates:
Data valid for the whole flight: weather data measured every hour: solar irradiance, windspeed, air temperature, air specific humidity; initial surface temperature at midnight and sub-surface temperature at lower boundary depth (0.50 m) (soil) and upper boundary height (air).

Data valid on a field by field basis: slope direction and slope dip; surface aerodynamic roughness; surface emissivity.

Data acquired pixel by pixel by the scanner: day and night surface temperatures; visible and near infra-red spectrometric measurements, combined to produce albedo values.

About the acquisition rate of the albedo values, it was verified in a preliminary study that, if the surface temperatures are to be used pixel by pixel, the same must be done for albedo which has a great importance in the surface heat balance entering in the Tell-us algorithm and which also varies pixel by pixel within a single field.

In the joint flight experiment the fields considered have very low or negligible slope dips so that this parameter, together with slope direction was not considered.

Surface aerodynamic roughness is another important parameter and the fields considered, where the Tell-us model is applicable or can at least be tested, have been grouped into three broad classes: ploughed bare soil with roughness estimated to 0.015 m; stubbles with roughness estimated to 0.020 m; burnt stubbles with roughness estimated to 0.010 m.

Emissivity should be, at best, measured for each field surface type. Such measurements, however, are not available for the flight over Grendon; it was estimated that the range of variation should be from 0.96 to 0.97 for the fields considered. As the model is hardly sensitive to this emissivity variation as separate input, a mean value of 0.965 was assumed for the whole area. As a result of this analysis, the procedure described in section 3.1 had to be enlarged in the following way:

- calculate with Tell-us a series of look-up tables by varying step by step albedo as input within suitable extrema;
- calculate this series of tables for as many input values of roughness as necessary (as done in the present case).

The following sequence of actions is then performed for each (Td, Tn, A) pixel of scanner data, A being albedo value:

- retrieve the field in which the given pixel is localized and the roughness value attributed to this field;

REPRODUCIBILITY OF THE
ORIGINAL PAGE IS POOR

- retrieve in the corresponding series the two tables with albedo input values on both sides of the A value;
- calculate THI and RSH from (Td, Tn) in each table as in section 3.1;
- determine the final THI and RSH values by linear interpolation between the two values calculated in the two tables;
- determine CDE as in section 3.1.

The retrieval of the corresponding field identity and roughness value implies that a file has been constructed in which all the pixels in each of the fields considered (and not in the other fields) are replaced by index values equal to the proper field number (field identity) and that a correspondence between field number and roughness value is available.

The various search and interpolating processes mentioned before, will thus work, within and between tables generated by the Tell-us algorithm, on a pixel by pixel basis with four "channels": day temperature, night temperature, albedo and field index.

Although the calculation of each of the tables by Tell-us can be rather time consuming in proportion to the accuracy requested (from a few seconds to a few minutes CPU time of IBM 370/165), the search and interpolating operations are very fast (19 min. for 312,000 pixels, i.e. 3.6×10^{-3} s per pixel) and allow the use of Tell-us with pixel by pixel input.

3.3 Mapping soil moisture and cumulative daily evaporation

Cumulative daily evaporation is obtained directly by the process mentioned before and then mapped point by point. Soil moisture percentage in the 0 - 15 cm upper layer is obtained by using the linear correspondence between thermal inertia and volumetric water content. Thermal inertia THI is indeed expressed as:

$$THI = \sqrt{\rho_c \cdot h_c}$$

where the heat capacity $\rho_c = [2(1 - \theta_s) + 4.2\theta] 10^6$ (J/m³/K) for not too high organic matter content [2], and the thermal conductivity $h_c = h_0 + (h_{0.5} - h_0) \frac{\theta}{0.5}$ (W/mK). θ is the volumetric moisture content, θ_s is the pore volume equal to 0.50 for the Oxford clay which is almost present everywhere in the fields of interest. h_0 and $h_{0.5}$ are the apparent thermal conductivities for $\theta = 0$ and $\theta = 0.5$ respectively, with values 0.75 and 1.4 (W/mK) [3]. It can be verified that in the practical range [$\theta = 0, \theta = 0.5$] THI depends linearly from θ with fairly good approximation.

4. CORRECTION OF THE SCAN ANGLE EFFECT ON THE SPECTROMETRIC VALUES

As the scan angle of the Daedalus instrument used for the flight is 77°, the variation of the atmospheric thickness along the scan line causes a variation in the atmospheric effect from the centre of the line towards the edges, with a resulting systematic effect in the data acquired, which must be corrected. Due to the difficulty to implement a deterministic correction scheme which requires an accurate knowledge of the physical phenomena as a function of angle, the statistical approach known as "along track averaging" was preferred and applied to thermal and visible data.

The method is known: all along the strip of acquired data, the mean values of the one pixel columns of data are calculated from edge to edge of the strip, a polynomial fitting of the mean values along the scan line attempts then to describe the general trend of the effect on the mean of the columns; if the effect is absent or negligible, the fitted curve results in a straight horizontal line. The difference between fitted curve and value at the central column element (nadir point) calculated at each column position, gives then the correction to be applied to the value of the element in this position, in every scan line.

In the present case, as a careful visualization of the data put in evidence a loss of contrast towards the edges, it was decided to correct also the variance in a similar way.

The correction curves exhibited a noticeable, although asymmetrical, effect on mean and variance for day thermal and visible data and on the mean for night thermal data, while the effect on the variance is almost negligible in the latter case. See Figs. 2a to 2d and in particular the strong asymmetry in Fig. 2c.

The mean and variance corrections were applied at the same time for each channel with the following formula:

$$x_{ij}^c = \bar{x}_0 + b_j(x_{ij} - \bar{x}_j)$$

where x_{ij} is the non-corrected value for element in scan line i and column j ; x_{ij}^c is the corrected value for the same element; \bar{x}_j is the value of the fitted curve of the means at column j ; \bar{x}_0 is the value of the mean at nadir (central column); b_j is the variance correction factor at column j calculated from the variance fitted curve.

REPRODUCIBILITY OF THE
ORIGINAL PAGE IS POOR

5. CORRECTION OF THE ATMOSPHERIC EFFECT AT NADIR POINT

The correction described above has the effect to give at each point the channel values it would have at nadir position from the air plane, in the centre of the scan line. The data must next be corrected from the effect due to the atmospheric layer at nadir.

5.1 Thermal data

The intention was to correct them by using the air temperature humidity and pressure data, acquired at various altitudes, in a model applying the radiative transfer equation to atmospheric layers. Unfortunately the data had to be collected rather far from the site (40 km apart) and the calculated corrections resulted to be very questionable.

Comparison with measurements made on the ground leads to the following situation:

- night temperature average values are very close to the corresponding average scanner values acquired over the same zone: $4.0 \pm 0.6^\circ\text{C}$ (PRT-5) instead of 4.1°C (Daedalus) for ploughed field and, similarly, 4.3 ± 0.4 and 4.8 for a field with a mixture of burnt and unburnt stubbles, 4.9 ± 0.5 and 5.65 for a tennis court, 5.2 ± 0.9 and 5.8 for a road crossing;
- two series of ground measurements were made for day temperatures with the same radiometer type (PRT-5) and at the same time approximately. The first series gave values systematically lower, from 2 to 5 and even 7° , than the scanner values for seven investigated places; it is, however, conjecturable that this could be due to a shortage in the power supplied by the portable batteries. The second series, where two places only were investigated, gave values in very good agreement with the scanner: 26.4 (PRT-5) instead of 26.8 (Daedalus) for ploughed field, 23.6 instead of 24.2 for grass of a sports field. Under such circumstances, where the atmospheric corrections for thermal data are difficult to be validly determined and likely to be rather small, it was decided not to take them into account, and to rely uniquely on the ground measurements. It is therefore desirable that atmospheric sounding be performed in situ in future campaigns.

5.2 Visible and near infra-red data

As the sky irradiance was measured from the ground by an Exotech 100 radiometer in the region from $0.50 \mu\text{m}$ to $1.1 \mu\text{m}$, only the channels 4 to 10 of the Daedalus scanner were used with relative band widths given in Table 1. It was assumed that the reflectance value for this wavelength range would be a reasonable approximation for the albedo value referred to the whole reflective range.

The atmospheric corrections were applied to each channel and the average reflectances of some fields were next calculated by using the sky irradiance value from the ground. The necessary calculations were obviously done to intercalibrate the two radiometers and to take into account their band width differences. These reflectances were then compared to the reflectances of the same fields measured on the ground. Details on the atmospheric corrections and the comparison between scanner and ground measured reflectances will be published later; a short outline will be sufficient for the present purpose.

The transmittance τ of each Daedalus channel which represents the atmospheric absorption factor, was estimated from the measurements made with the Exotech radiometer with a visibility of about 18 km and corrected for the scanner altitude by the factor $\tau_{1000}/\tau_{\infty}$ calculated with the Turner model [4].

The additive path radiance term L_p for each channel was also obtained from the Turner model with 18 km visibility and corrected for the scanner altitude with data obtained from the LOWTRAN model [5].

Both τ and L_p factors are displayed in Table 1; as L_p depends on the surface albedo, the values are given for the three soil surfaces investigated, they were calculated from ground measured reflectances. As it is seen, they are very close to each other, so that an average value over burnt and unburnt stubbles (more often found among the investigated fields), could be used everywhere to simplify the calculations. The reflectance is calculated by the following formula [6]:

$$I = \frac{\pi}{\sum_{i=4}^{10} \Delta\lambda_i} \int_{\lambda=4}^{10} \left(\frac{P_i}{A\Omega} - L_{p_i} \right) \frac{1}{\tau_i}$$

where τ_i and L_{p_i} are respectively the transmittance and path radiance for channel i ; P_i is the power received by the radiometer in channel i , calculated through the calibration coefficients, from the data of channel i ; I is the sky irradiance for channel i measured from the ground; A is the area of the ground seen through the IFOV of the scanner; Ω is the effective optical aperture of the radiometer.

REPRODUCIBILITY OF THE ORIGINAL PAGE IS POOR

As a global result, the comparison is the following, between ground measured reflectances and scanner measured reflectances corrected from atmospheric effect:

- ploughed field - bare soil: 0.085 (ground) and 0.090 (scanner);
- burnt stubble field: 0.048 and 0.055;
- field with mixture of burnt and non-burnt stubbles: 0.068 and 0.082.

They are in both cases average values over the corresponding field. The discrepancies range from 6 to 20%, which is still acceptable by considering that the Tell-us algorithm is hardly sensitive to such albedo variation. Variations above 40 or 50%, which occur from field to field and often within the same field, must however be taken into account. Decreasing the albedo in input from 0.1 to 0.05 for instance has the effect to increase by about 10% thermal inertia and soil moisture in output.

6. CORRECTION FOR THE SURFACE EMISSIVITY

The surface emissivity ϵ is used to pass from radiative temperature T_r , measured by the ground or the aircraft radiometer, to the actual temperature T , with the help of the formula $T = T_r \epsilon^{-\frac{1}{4}}$ derived from the Stefan-Boltzmann radiation law. The ϵ value varies with each field surface but as measurements are not available for the Grendon experiment and estimates of ϵ give a variation which is likely to be in the range of 0.96 to 0.97 for the fields of interest here, a constant average value of 0.965 was assumed for all the fields. This results in an increase of the measured temperatures by 0.9% ($^{\circ}\text{K}$).

7. REGISTRATION OF NIGHT THERMAL DATA OVER DAY THERMAL AND VISIBLE DATA

Day thermal and visible data are automatically registered for they were acquired during the same flight through the same instrument optics and with the same resolution, 2.5 m at 1000 m altitude. Night thermal data acquired during a previous flight, have the same resolution but they must be superposed by software to day data.

7.1 The method used

The problem is to map the grid of night data on the grid of day data. This is obtained by using bivariate polynomials as mapping functions [7]. A pixel with coordinates (x, y) , given by the line and column position, in the day data, is thus the transformed element from a pixel with coordinates (u, v) in the night data such that:

$$u = u(x, y) = \sum_{p=0}^N \sum_{q=0}^P a_{pq} x^p y^q$$

$$v = v(x, y) = \sum_{p=0}^N \sum_{q=0}^P b_{pq} x^p y^q$$

REPRODUCIBILITY OF THE ORIGINAL PAGE IS POOR

where u and v are calculated from x and y .

In the present case second order polynomials were chosen. The method uses ground control points which are common to day and night data to determine the a_{pq} and b_{pq} coefficients by least square fitting. The fitting of the ground control points is performed in the untransformed grid (night data), rather than in the transformed grid (day data), as would seem more natural. The latter solution would indeed require to express the (x, y) coordinates as a function of the (u, v) , i.e. to reverse the preceding expressions. The calculated (u, v) coordinates will not be generally integer and the nearest neighbour rule is applied to determine the pixel radiometric value. This simple procedure has been preferred in the present case to interpolation or convolution methods, in consideration of the average accuracy of the registration which in any case cannot guarantee less than two pixels.

As the complete strip of data is rather long (more than 4000 lines of 672 pixels), the registration is made for successive blocks of 672 x 300 points with 50% overlapping; 12 to 20 control points by block determine the respective pair of transformation polynomials. Discontinuities between blocks are avoided by combining with variable weights the coefficients of the polynomials referring to two successive blocks. As the line of data processed moves from the centre of the first block to the centre of the second block, the weights relative to the first pair of polynomials are changed line by line from 1 to 0, the reverse being done for the second pair. The process is then repeated with the second and third blocks and so on.

7.2 The results obtained

They are displayed in Fig. 4. The average registration error between ground control points was found to be 2.3 pixels with minimum 0 and maximum 7 pixels. The average registration error on the other points is not known but is very likely to have a similar value in this case of low order transformation polynomials.

8. RESULTS - SOIL MOISTURE AND EVAPORATION MAPS

8.1 Simulated night temperatures

As already said, the process set up here uses a series of look-up tables generated by the Tell-us model. For each table, Tell-us simulates T_d and T_n values which must fit with the various input parameters (weather data, albedo, etc.) and with a set of values of THI and RSH. In order to save computing time in the calculation of the 57 necessary tables, a fast version of Tell-us was run which uses a somewhat high heat capacity to allow calculation time steps of one hour (instead of 2 to 5 minutes for the slow version which requires 5 minutes machine time per table). As a result, the simulated T_n values are systematically lower by about 1.5° . A second systematic effect derives from the very low wind speed during the night; earlier experiments have indeed shown that the simulated T_n falls down below measured values from about 1° in this situation. The conclusion was then to increase the simulated T_n values by 2.5° while waiting for a solution of the above problems by improvements on the calculation scheme and on the model.

8.2 Thermal inertia and soil moisture

All mapped results are relevant to the fields for which Tell-us is presumably applicable. Compare for illustration Figs. 3 to 5 and Figs. 6 to 10. Vegetated zones like meadows, forests, standing cereal crops were not considered.

Fig. 9 is the display of both thermal inertia and soil moisture mapped in 6 classes of thermal inertia soil moisture. The soil moisture measurements available for our purpose were done only in the ploughed field and gave a mean value of 0.30 ($\pm \sigma = 0.024$) water content by weight determined over 8 core samples taken at 15 cm depth. The mean value of soil moisture calculated by Tell-us over the whole field is 0.22 ± 0.03 by volume which corresponds to 0.21 ± 0.02 by weight, assuming a density of 1.1 for the 15 cm top soil layer. The calculated value is 30% lower but this comparison, although it is indicative for a tendency, should be considered with some caution; first because the moisture content of the core sample at 15 cm depth is not likely to be identical to the moisture content of the 15 cm top layer, second because the correspondence between thermal inertia and soil moisture leaves somewhat undetermined the depth of the top layer concerned and third because the top layer density is not known exactly and could vary from 1.0 to 1.2.

A comparison was made with apparent thermal inertia P calculated with NASA-HCMM formula [8], expressed as $P = C(1 - a)/(T_d - T_n)$, where a is the albedo and C is a constant which, in the present case, has been determined in order to fit with the mean values for the ploughed field of T_d , T_n and THI calculated by Tell-us. The results are displayed in Fig. 8 with class limits identical to those used in Fig. 9. As expected, the mapping inside the ploughed field is almost identical in the two figures. One can see that the general trends are roughly the same in the other fields. The detailed variations differ noticeably however, although to a minor degree for the fields towards the left side. Further investigations should consequently examine the possibility to approximate the Tell-us model with the help of such a simple formulation under well controlled and well calibrated conditions.

8.3 Cumulative daily evaporation

The mapped results obtained with Tell-us are displayed in Fig. 10. It is seen that CDE varies roughly in the same direction as THI and soil moisture which is reasonable. The detailed behaviour of CDE is however more complex because of the role played by RSH in the look-up tables. Two fields have for instance higher mean values of CDE than the three fields located between them (towards the left side of Fig. 10), although having about the same average THI value as the latter; this is due to much higher RSH values, on the average, for the two fields.

Evaporation is, on the other hand, estimated to be zero (or negative which means condensation) in some zones, for 8% of the total area. As condensation did not actually occur during the flight experiment, one must conclude that low range evaporation is not well calculated by the model.

Limiting values of CDE have been calculated with the "Tergra" model [9] for volume moisture content of 0.44 (i.e. THI = 1940) and RSH = 1.0; they are compared in Table 2 to the Tell-us values which are lower by about 10%.

8.4 Local behaviour of moisture and evaporation

As will be seen by comparing Figs. 9 and 10 with Fig. 3, the detailed mapped results for some fields are influenced by the pixel by pixel variation of T_d , which is not likely to occur really, as soil moisture and evaporation will vary more slowly. This effect is stronger for non-homogeneous field surfaces made of variable mixtures of burnt and unburnt stubbles or cropped cereals. In these cases there is also a strong variation of aerodynamic roughness on a pixel by pixel basis. The model is very sensitive to these variations: doubling the roughness has the effect to modify by 1 to 3% the simulated day and night temperatures. In such difficult situations, the mapping of moisture and evaporation would then require that further to albedo, also roughness be acquired and taken into account on a pixel by pixel basis, which is hardly feasible at the present stage. A possible solution could be to smooth the effect by averaging over superpixels, if one agrees, however, to the corresponding loss of detailed information.

9. CONCLUSIONS

From the point of view of data processing it has been verified that a detailed mapping of thermal inertia, soil moisture and evaporation is possible with day and night thermal and albedo data acquired by air borne scanner, and by using a rather complex model like "Tell-us" which reverses a temperature simulation process.

The comparison with measured values is subject to uncertainties but it seems to indicate a tendency of the model to underestimate moisture content. Other measurements would be necessary to check the results on a more reliable basis. The same can be said for cumulative daily evaporation for which no measurement was available; the above mentioned tendency is however also verified.

In inhomogeneous areas, where temperature, albedo and surface roughness vary rapidly, these rapid variations tend to mask partially the more smoothed evolution of moisture and evaporation, as long as roughness is not taken into account pixel by pixel, as was done for albedo.

Acknowledgements

The authors would like to thank Dr. K. Blyth and Dr. R.J. Gurney, Institute of Hydrology, Wallingford, U.K., for permitting the use of some of their measurements performed during the joint flight experiment.

References

- [1] A. Rosema and J.H. Bultveld, P. Reiniger and G. Tassone, K. Blyth and R.J. Gurney, "Tell-us", a combined surface temperature, soil moisture and evaporation mapping approach. 12th Int. Symp. on Remote Sensing of Environment, Manila, Philippines, 20-26 April, 1978.
- [2] D.A. De Vries, Heat Transfer in Soils. In: D.A. De Vries and N.H. Afgan, Heat and Mass Transfer in the Biosphere, Part II: Transfer Processes in the plant environment. Scripta Book Company, Washington D.C., 1975.
- [3] R.A. Feddes, Some physical aspects of heat transfer in soil. Miscellaneous reprints no 145 of the Institute for Land and Water Management Research, Wageningen, The Netherlands, 1973.
- [4] R. Turner, M. Spencer, Atmospheric model for correction of spacecraft data. Proc. 8th Int. Symp. on Remote Sensing of Environment, Ann. Arbor, Michigan, 1972.
- [5] J.E.A. Selby, R.A. McClatchey, Atmospheric transmittance from 0.25 to 28.5 μm : Computer code LOWTRAN 3. Air Force Cambridge Research Lab., Massachusetts, 1975.
- [6] R.W. Preisendorfer, Radiative transfer on discrete spaces. Pergamon Press, 1965.
- [7] R. Bernstein, Digital Image Processing of Earth Observation Sensor Data. IBM Journal of Research and Development, 1, 1976.
- [8] Data utilization plan for Applications Explorer Mission - A, HCMM. G.S.F.C. Greenbelt, Maryland, 10 1977.
- [9] G.J.R. Smit, The Tergra model, a mathematical model for the simulation of the daily behaviour of crop surface temperature and actual evapotranspiration, Niwars publ. 46, Delft, The Netherlands, 1977.

REPRODUCIBILITY OF THE
ORIGINAL PAGE IS POOR

Table 1: Path radiance and transmission used to correct the Dandelion reflective data from atmospheric effects

Dandelion channels	Path radiance (m ² cm ⁻² steradians)	Path radiance (m ² cm ⁻² steradians)			Transmission for altitude 1000 m	
		Stables	Burnt stables	Bare soil		
4	0.50-0.55	0.040	0.530	0.042	0.0395	0.85
5	0.55-0.60	0.032	0.831	0.033	0.0315	0.89
6	0.60-0.65	0.027	0.926	0.029	0.0265	0.90
7	0.65-0.69	0.018	0.917	0.019	0.0175	0.88
8	0.70-0.79	0.032	0.930	0.033	0.0310	0.89
9	0.80-0.89	0.023	0.821	0.024	0.0220	0.87
10	0.92-1.10	0.027	0.923	0.029	0.0250	0.83

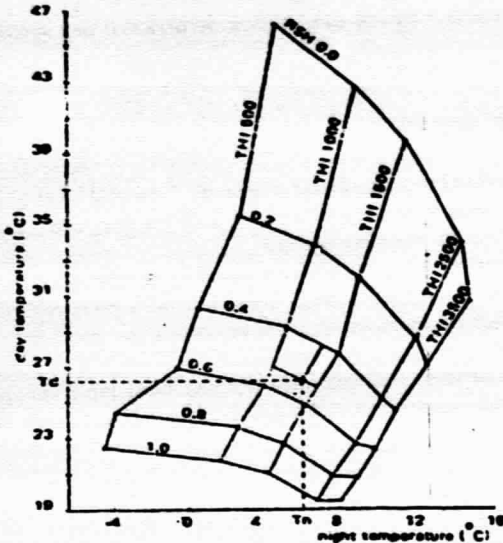


FIG. 1a

Table 2: Cumulative daily evaporation calculated by Tergo and Tell-us models for volume moisture content 0.66 and relative surface humidity 1.0

Aer. Roughness (m)	ALBEDO	CDE Tergo (mm)	CDE Tell-us (mm)	Difference %
0.010	0.07	2.30	2.07	10
0.020	0.07	2.45	2.29	7
0.010	0.14	2.12	1.85	13
0.020	0.14	2.29	2.06	10

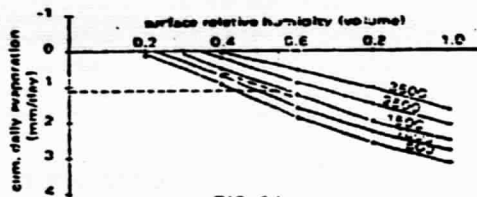


FIG. 1b

Fig. 1: Look-up graphs calculated by Tell-us in the case of bare soil with albedo 0.09

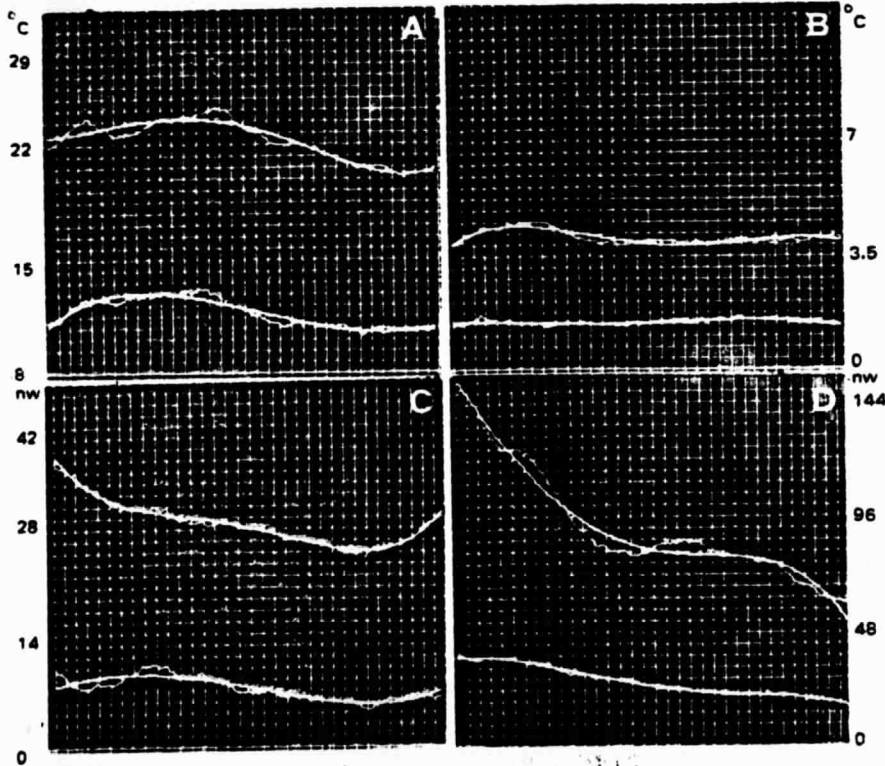


Fig. 2: Correction curves to remove the scan angle effect on spectrometric values. Upper curves: variation of the column mean and relative fitted curve along the scan line. The same or variances in the lower curves. Four channels only are represented: day thermal (2a), night thermal (2b), channel 5 (2c) and channel 10 (2d).

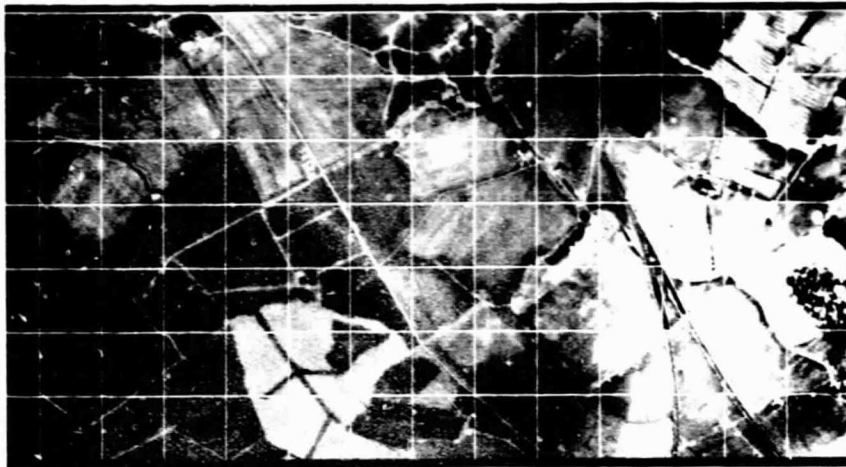


Fig. 4a: Mapped night temperatures, original data. Range of variation $0^{\circ}\text{C} - 18^{\circ}\text{C}$ (radiative values).

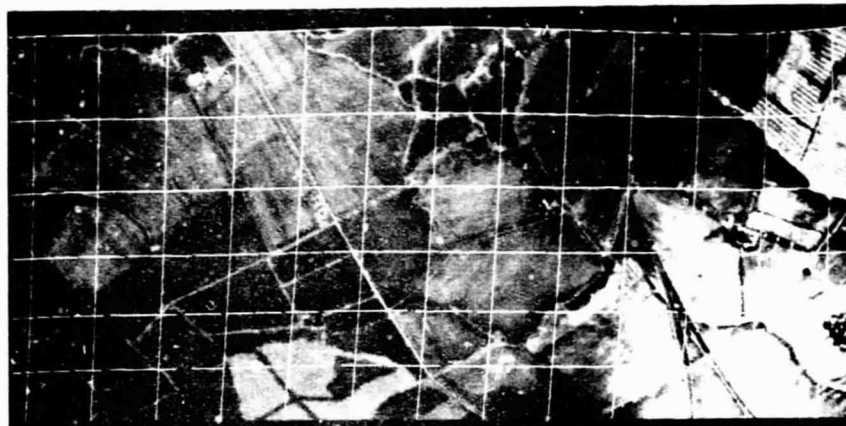


Fig. 4b: Mapped night temperatures. Data geometrically corrected. The transformation is visible through the grid deformation.

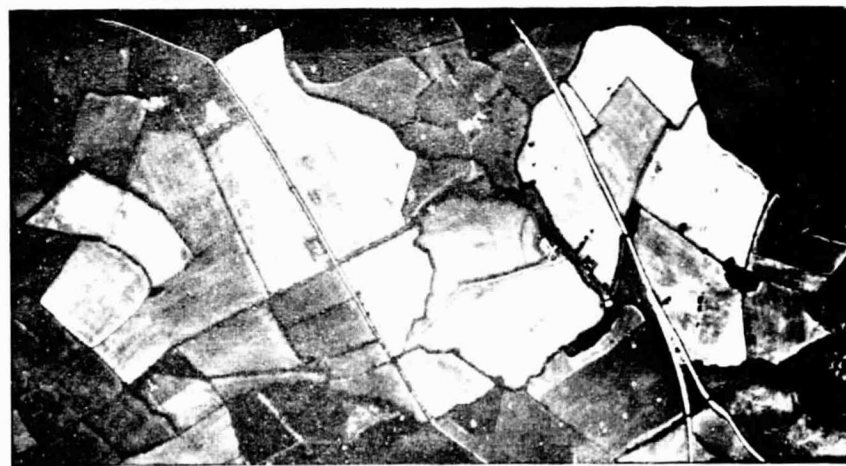


Fig. 3: Mapped day temperature. Range of variation $8^{\circ}\text{C} - 44^{\circ}\text{C}$ (radiative values)



Fig. 5: Mapped albedo values. Range of variation 0.02 - 0.20 in the investigated fields.

REPRODUCIBILITY OF THE ORIGINAL PAGE IS POOR

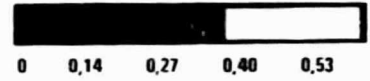
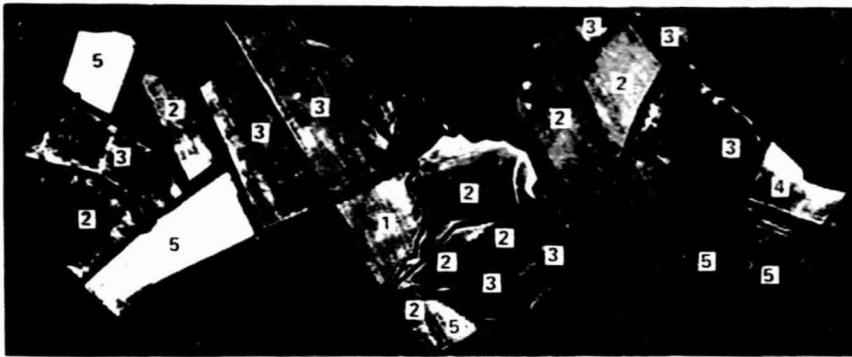


Fig. 10: Cumulative daily evaporation calculated by Tell-us and mapped in 5 grey levels (mm). 1: bare soil; 2: stubbles; 3: burnt & unburnt stubbles; 4: stubbles with green shoots; 5: stubbles & cropped cereals.

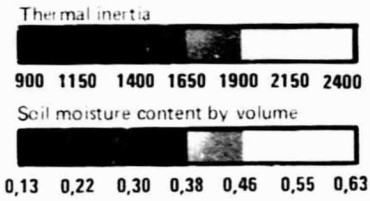


Fig. 9: Thermal inertia and soil moisture calculated by Tell-us and mapped in 6 grey levels.

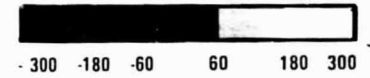


Fig. 7: Difference between Fig. 9 and Fig. 8 mapped in 5 grey levels.



Fig. 8: Apparent thermal inertia mapped in 6 grey levels.

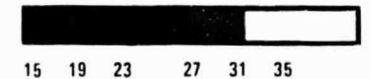


Fig. 6: Temperature differences ($T_d - T_n$) mapped in 6 grey levels.

REPRODUCIBILITY OF THE ORIGINAL PAGE IS POOR